International Journal of Medical, Medicine and Health Sciences
ISSN: 2517-9969
Vol:15, No:9, 2021

Automated 3D Segmentation System for Detecting Tumor and Its Heterogeneity in Patients with High Grade Ovarian Epithelial Cancer

D. A. Binas, M. Konidari, C. Bourgioti, L. Angela Moulopoulou, T. L. Economopoulos, G. K. Matsopoulos

***Abstract*—**High grade ovarian epithelial cancer (OEC) is the most fatal gynecological cancer and poor prognosis of this entity is closely related to considerable intratumoral genetic heterogeneity. By examining imaging data, it is possible to assess the heterogeneity of tumorous tissue. This study presents a methodology for aligning, segmenting and finally visualizing information from various magnetic resonance imaging series, in order to construct 3D models of heterogeneity maps from the same tumor in OEC patients. The proposed system may be used as an adjunct digital tool by health professionals for personalized medicine, as it allows for an easy visual assessment of the heterogeneity of the examined tumor.

***Keywords*—**K-means segmentation, ovarian epithelial cancer, quantitative characteristics, registration, tumor visualization.

I. Introduction

ONE of the most dangerous types of cancer for female population is high grade OEC. In fact, OEC is the fourth most common gynecological malignancy worldwide and the most fatal one, accounting for over 70% of deaths among patients with ovarian carcinoma [1], [2].

In patients with OEC, the presence of intratumoral genetic heterogeneity is considered an important adverse prognostic factor associated with poor response to treatment and, therefore, poor survival rates. The heterogeneity of tumorous tissue can be assessed through the use of medical imaging data and in particular Magnetic Resonance Imaging (MRI). MRI is widely used as a problem-solving imaging modality for the evaluation of adnexal lesions due to its increased soft tissue resolution [3], [4]. Functional MRI techniques, such as diffusion weighted imaging (DWI), may be used to assess tumor cellularity, as in general, highly cellular tissues exhibit lower apparent diffusion coefficients (ADC).

The aim of this study is to present a complete visualization system for evaluating intratumoral genetic heterogeneity of extracted cancerous areas of interest through modeled 3D images, by using multiple imaging sequences, in search of differences in histological and genetic data, which may subsequently affect prognosis and treatment.

D. A. Binas and G. K. Matsopoulos are with the School of Electrical and Computer Engineering, National Technical University of Athens, Athens, Greece (e-mail: jimbin4@gmail.com, gmatso@esd.ece.ntua.gr).

M. Konidari MD, C. Bourgioti MD, and L. A. Moulopoulos MD are with the Department of Radiology, National and Kapodistrian University of Athens, Athens, Greece (e-mail: marianna_konidari@hotmail.com, charisbourgioti@yahoo.com, lmoulop@med.uoa.gr).

T. L. Economopoulos is with the School of Electrical and Computer Engineering, National Technical University of Athens, Athens, Greece (corresponding author, e-mail: theodore@biomig.ntua.gr).

II. Methodology

A. Data Acquisition

Between March 2019 and September 2019, 10 women with clinical and laboratory findings suspicious of OEC underwent dedicated pelvic MRI in the Department of Radiology (blinded) at Aretaieion Hospital. None of the patients had received any surgical or conservative treatment for OEC and none of them had any contraindication for MRI.

All MRI acquisitions were performed using a 3.0T magnet unit (Philips Healthcare, Best, The Netherlands). The MRI protocol designed for this study included the following sequences:

1) T2 weighted -DIXON (axial plane)
2) DWI-STIR (axial plane)
3) DWI-STIR-ADC (axial plane)

B. Algorithm

The proposed methodology for visualizing the heterogeneity of the detected cancerous region of interest depends solely on image processing techniques, which are applied to three specific imaging series from the aforementioned MRI dataset, namely, T2 weighted, DWI and DWI ADC. The methodology itself comprises of the following discrete steps: (a) alignment of the processed imaging series, (b) detection of the outline of the cancerous region, (c) superimposition (fusion) of images for projecting the required imaging information onto the cancerous region. In order to achieve this, the developed image processing system includes the following subsystems:

1) Image registration subsystem
2) Image segmentation subsystem
3) Image fusion subsystem

The overall processing flow of the proposed system is presented in Fig. 1.

Initially, the imaging sequences from the T2 weighted and DWI (for $b = 0$) series are aligned, using a two-stage registration technique. In general, image registration can be defined as the spatial alignment of an imaging data set (moving), with respect to a reference data set, through a repetitive process which calculates the parameters of a geometrical transformation, according to a preferred optimization algorithm and a measure of match [5]. In the case of this study, an initial fast registration was performed, using the Affine transformation, Downhill Simplex as the preferred

optimization method and the Mattes Mutual Information as a measure of match [6], [7]. Then, a second, thorough registration step is performed, based on the non-rigid Demon algorithm, which freely deforms the moving imaging data through the definition of a deformation field [8]. Since there is no spatial difference between the b-value subseries of the DWI dataset, the result of the above registration scheme is the alignment of the entire DWI series (for all b-values) to the T2 weighted images. The same approach is applied for aligning the DWI ADC images to the T2 weighted series.

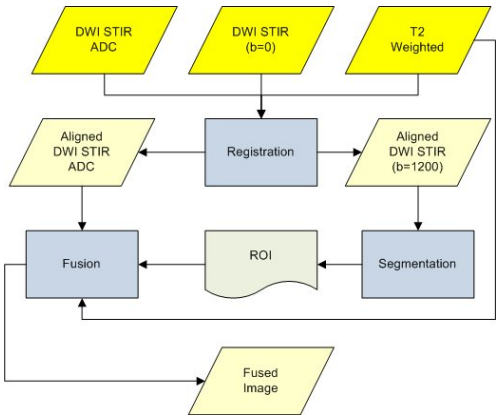

Fig. 1 Flow Diagram of the Proposed System

Once the required data sets are properly aligned, the cancerous region of interest may be extracted from the DWI series and specifically from the images acquired for *b = 1200*. For this purpose, the K-Means clustering approach was preferred. Particularly, K-means considers the pixels of an image as a set of *n* data points, which are classified according to the mean squared distance of those points from a set of predefined points, called centers, which define the centroids of a predefined number of classes (clusters). Classification is achieved through the minimization of the mean squared distance of each data point to its nearest center point. After classifying all image pixels into tumorous/non-tumorous, the outline of the cancerous region could be defined.

The final step of the proposed methodology involves the combination of information from the T2 weighted imaging data and the outlined cancerous region extracted from the previous step, as well as the partitioning of the tumor in homogenous areas. This can be achieved using image processing techniques generally referred to as "Image Fusion". In the first case, the intensity values from the aligned extracted cancerous region of interest are superimposed on the T2 weighted data. In order to depict the heterogeneity of the tumor, the ADC values extracted from the aligned DWI ADC data set are considered. ADC is a measure of the magnitude of diffusion of water molecules within the tissue, and it is closely related to tissue cellularity. The lower the ADC value, the higher the diffusion restriction (and cellularity) of the tissue. Specifically, a three-color scheme was employed, based on cutoff ADC values provided by two experienced genitourinary radiologists:

1) blue color for values > 1.2 x 10^{-3} mm^2/sec,
2) yellow color for values between 0.85 x 10^{-3} mm^2/sec and 1.2 x 10^{-3} mm^2/sec,
3) red color for values <0.85 x 10^{-3} mm^2/sec.

Both visual entities, namely the fused DWI and T2 weighted intensities, as well as the heterogeneity maps, based on the ADC data, are composed into respective 3D models and visualized through an appropriate graphical user interface.

The proposed system is designed to provide users with the ability to change the method of segmentation and to select specific MRI sequences for superimposition (fusion). Particularly, several methods of segmentation techniques have been tested, such as K-Means, Watershed [9], Dual Thresholding, Otsu and Region Growing, to finally conclude that optimal segmentation results were provided using the K-Means algorithm [10]. The built-in visualization tool supports the rotation/zooming of the extracted tumor model, as well as the ability to export and recall the depicted images at any time.

All image processing routines were developed using the Insight Toolkit (ITK) [11]. The resulting 3D models were visualized through the Visualization Toolkit (VTK) [12].

III. Results

Data from all 10 MRI data sets were processed to produce respective 3D models of the tumors in each case. The estimated 3D models were assessed through visual inspection, as well as by quantifying the heterogeneity of the extracted tumors.

A. Qualitative Results

Some examples of the obtained 3D models are presented in Figs. 2-7. In particular, Figs. 2, 4 and 6 show the extracted tumor projected to the T2 weighted imaging data. In Figs. 3, 5, and 7, tumor heterogeneity is presented using a three-color scheme: red color for low ADC values, yellow color for intermediate ADC values and blue color for high ADC values. In all cases, the tumor outline is clearly seen, as well as the body of the patient, as extracted from the T2 weighted imaging sequence.

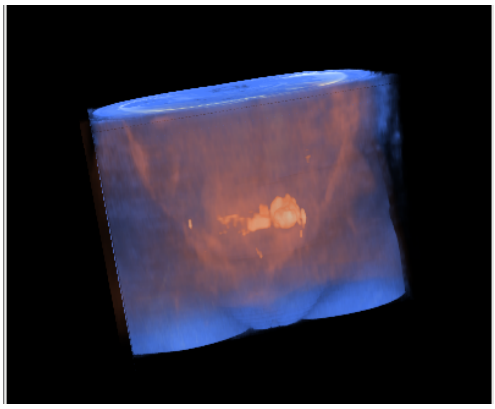

Fig. 2 OEC segmentation result (from DWI with b = 1200) superimposed to the patient's body (T2 weighted) (Patient 6)

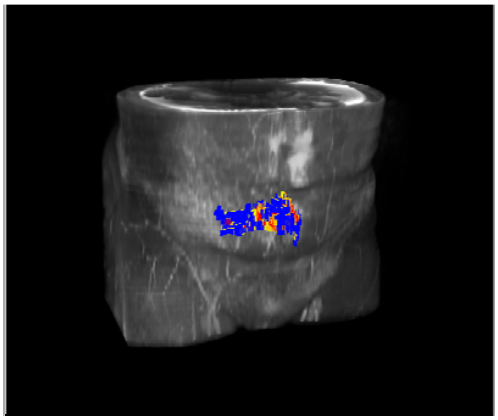

Fig. 3 OEC tumor projected with intratumoral areas of different ADC values (Patient 6)

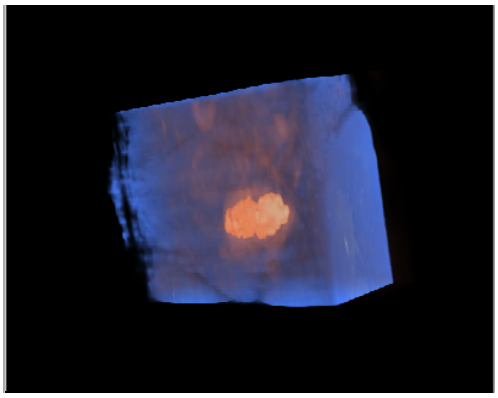

Fig. 4 OEC segmentation result superimposed on the patient's body (Patient 12)

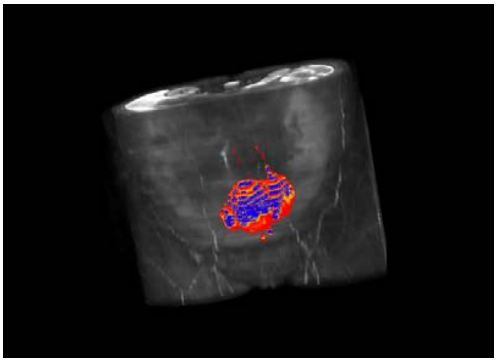

Fig. 5 OEC projected with intratumoral areas of different ADC values (Patient 12)

B. Quantitative Results

Table I illustrates the number of pixels and corresponding percentages of high (blue), intermediate (yellow) and low (red) ADC values in the anatomy of the T2 data. In all cases, yellow areas correspond to the transition of ADC values from high to low (or the opposite) and thus present an intermediate state of recorded ADC measurements.

On average, the entire processing pipeline required 1-3 minutes (depending on the processed data sets). All tests were performed on a common reference system (Intel Xeon E5-1620v4 at 3.5 GHz, 32 GB of RAM, running on Debian 10 GNU/Linux).

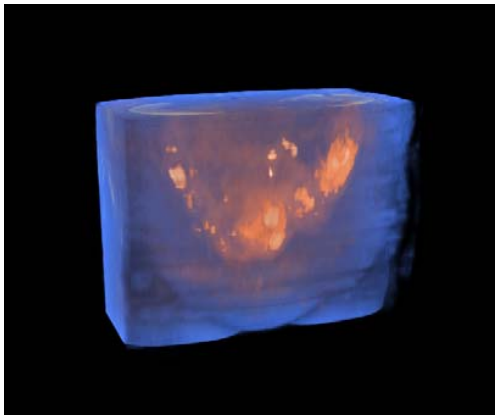

Fig. 6 OEC segmentation result superimposed on the patient's body (Patient 22)

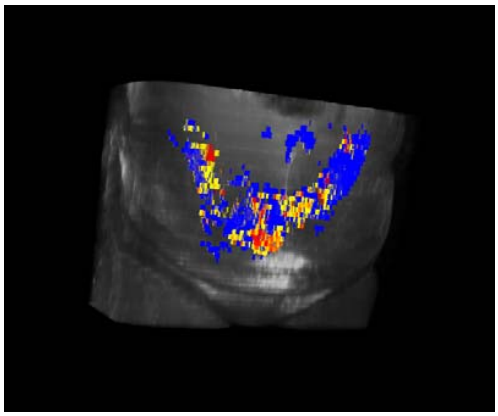

Fig. 7 OEC projected with intratumoral areas of different ADC values (Patient 22)

TABLE I
QUANTITATIVE RESULTS

Patient	Number of pixels			Percentage (%)		
	Blue	Yellow	Red	Blue	Yellow	Red
6	1501	990	2171	32,2	21,24	46,57
12	16605	8035	1254	64,13	31,03	4,84
16	35580	38487	288	47,85	51,76	0,39
18	32411	27613	7118	48,27	41,13	10,6
22	20699	17265	12053	41,38	34,52	24,1
23	30383	1202	383	95,04	3,76	1,2
27	18015	1416	115	92,17	7,24	0,59
28	60192	896	881	97,13	1,45	1,42
29	74829	7642	111	90,61	9,25	0,13
30	23241	1246	297	93,77	5,03	1,2

IV. DISCUSSION

The presented qualitative and quantitative results demonstrate that the proposed system is a flexible tool for detecting ovarian tumor and for visualizing intratumoral heterogeneity. A basic step to achieve this is the precise

segmentation of the region of interest (tumor). As mentioned, the methods tested with satisfying results are K-Means, Watershed, Otsu and Dual Threshold. In order to optimize the parameters of each of the above methods, several trials were performed and the segmentation results in each case were validated against manually extracted regions of interest, provided by an experienced genitourinary radiologist, using the kappa statistic as a quantitative metric [13].

As mentioned, the K-means method provided the overall best results with the same parameters for every patient, thus allowing for a mostly automated segmentation scheme. The proposed system also provides the ability for 3D-printing, as it is able to export the depicted 3D models in various popular formats supported by most 3D printers. This can be particularly useful to surgeons, as by examining a 3D printed model of the tumor they can easily select suitable tissue samples from the tumor (red/blue areas) for further genetic analysis. Identification of intratumoral genetic heterogeneity may help identify areas of unsuspected, more aggressive tumor and thus select the appropriate therapy for the individual patient (personalized medicine).

Another area for possible future work is to develop a fully automatic segmentation method using, for example, U-Nets or a Geodesic Active Contours technique, or even a combination of the simpler methods currently supported by the system.

The ultimate goal of this study is the development of a decision support system for the prediction of OEC aggressiveness, using neural networks, based on features derived from morphological and functional MRI sequences. According to the presented results, the developed system presented in this paper is an initial step towards this direction.

V. Conclusion

A complete methodology for assessing OEC cases was presented in this study, based on the visualization of the heterogeneity of the cancerous tissue. The proposed methodology involves the use of advanced image processing techniques for aligning MRI datasets, for isolating cancerous regions and finally for reconstructing 3D models presenting heterogeneity maps. Those maps can be very useful to health professionals for assessing the level of severity associated with various parts of the tumor and hence devising an optimal therapeutic scheme.

Acknowledgment

This research has been co-financed by the European Union and Greek national funds through the Operational Program Competitiveness, Entrepreneurship and Innovation, under the call RESEARCH–CREATE–INNOVATE (project code: T1EDK-02886).

References

[1] S. A. Cannistra, “Cancer of the Ovary,” *N. Engl. J. Med.*, vol. 351, no. 24, pp. 2519–2529, Dec. 2004, doi: 10.1056/NEJMra041842.

[2] D. D. Bowtell et al., “Rethinking ovarian cancer II: Reducing mortality from high-grade serous ovarian cancer,” *Nature Reviews Cancer*, vol. 15, no. 11. Nature Publishing Group, pp. 668–679, Oct. 23, 2015, doi: 10.1038/nrc4019.

[3] L. R. Medeiros et al., “Accuracy of magnetic resonance imaging in ovarian tumor: A systematic quantitative review,” *Am. J. Obstet. Gynecol.*, vol. 204, no. 1, pp. 67.e1-67.e10, 2011, doi: 10.1016/j.ajog.2010.08.031.

[4] E. Sala, S. Wakely, E. Senior, and D. Lomas, “MRI of malignant neoplasms of the uterine corpus and cervix,” *American Journal of Roentgenology*, vol. 188, no. 6. AJR Am J Roentgenol, pp. 1577–1587, Jun. 2007, doi: 10.2214/AJR.06.1196.

[5] L. G. Brown, “A survey of image registration techniques,” *ACM Comput. Surv.*, vol. 24, no. 4, pp. 325–376, Jan. 1992, doi: 10.1145/146370.146374.

[6] D. Mattes, D. R. Haynor, H. Vesselle, T. K. Lewellen, and W. Eubank, “PET-CT image registration in the chest using free-form deformations,” *IEEE Trans. Med. Imaging*, vol. 22, no. 1, pp. 120–128, Jan. 2003, doi: 10.1109/TMI.2003.809072.

[7] S. Raghunathan, P. Schmalbrock, and B. D. Clymer, “Image Registration Using Rigid Registration and Maximization of Mutual Information" in *The 13th Annual Medicine Meets Virtual Reality Conference*, 2005.

[8] J. P. Thirion, “Image matching as a diffusion process: An analogy with Maxwell’s demons,” *Med. Image Anal.*, vol. 2, no. 3, pp. 243–260, Sep. 1998, doi: 10.1016/S1361-8415(98)80022-4.

[9] W. E. Higgins and E. J. Ojard, “Interactive morphological watershed analysis for 3D medical images,” *Comput. Med. Imaging Graph.*, vol. 17, no. 4–5, pp. 387–395, 1993, doi: 10.1016/0895-6111(93)90033-J.

[10] T. Taxt, A. Lundervold, B. Fuglaas, H. Lien, and V. Abeler, “Multispectral analysis of uterine corpus tumors in magnetic resonance imaging,” *Magn. Reson. Med.*, vol. 23, no. 1, pp. 55–76, Jan. 1992, doi: 10.1002/mrm.1910230108.

[11] “ITK | Insight Toolkit.” https://itk.org/ (accessed May 05, 2021).

[12] VTK - The Visualization Toolkit.” https://vtk.org/ (accessed May 05, 2021).

[13] A. P. Zijdenbos, B. M. Dawant, R. A. Margolin, and A. C. Palmer, “Morphometric analysis of white matter lesions in MR images: method and validation.,” *IEEE Trans. Med. Imaging*, vol. 13, no. 4, pp. 716–24, 1994, doi: 10.1109/42.363096.